Research Square

Preprints are preliminary reports that have not undergone peer review.
They should not be considered conclusive, used to inform clinical practice,
or referenced by the media as validated information.

HOXD11 promotes lung adenocarcinoma progression by transcriptionally activating CREB5 and enhancing AKT/mTOR signaling

Jiahong Han
China Medical University
Changrui Jiang
China Medical University
Yuanjie Zhang
China Medical University
Yunfeng Jiang
China Medical University
Jun Ye
China Medical University
Liandong He
China Medical University
Jiajun Wang
China Medical University
Shun Xu
xscmu1st@163.com
China Medical University

Research Article

Keywords: Lung adenocarcinoma, Transcriptional regulation, HOXD11, Tumor progression, Therapeutic target, ChIP-seq

Posted Date: November 3rd, 2026

DOI: https://doi.org/10.21203/rs.3.rs-8101552/v1

License: This work is licensed under a Creative Commons Attribution 4.0 International License.
Read Full License

Additional Declarations: No competing interests reported.

Abstract

Background

Lung adenocarcinoma (LUAD) is one of the most prevalent and lethal forms of lung cancer globally. Understanding the molecular drivers of LUAD progression is critical for developing targeted therapies. Although HOX family transcription factors are known contributors to oncogenesis, the role of HOXD11 in LUAD remains unexplored.

Methods

Comprehensive in vitro and in vivo assays were employed to evaluate the function of HOXD11 in LUAD. Transcriptomic profiling (RNA-seq), chromatin immunoprecipitation sequencing (ChIP-seq), and bioinformatic analyses were used to identify downstream targets. The impact of HOXD11 and its downstream effector CREB5 on LUAD cell growth, migration, and invasion was assessed through RNA interference, overexpression strategies, EdU incorporation, colony formation, Transwell, and scratch assays. Xenograft models in nude mice were used to validate tumorigenic potential. Protein and transcript levels were analyzed by Western blot and qRT-PCR, and immunohistochemistry was performed on tumor sections.

Results

HOXD11 expression was markedly elevated in LUAD tissues and cell lines and correlated with poor prognosis. Functional assays demonstrated that HOXD11 enhances LUAD cell proliferation, migration, and invasion in vitro and accelerates tumor growth in vivo. Mechanistic studies identified CREB5as a direct transcriptional target of HOXD11, as confirmed by ChIP-seq and luciferase reporter assays. CREB5 knockdown significantly abrogated the oncogenic effects of HOXD11. Moreover, the HOXD11-CREB5 axis was found to directly activate the AKT/mTOR signaling pathway, contributing to aggressive tumor behavior.

Conclusion

Our findings uncover a novel regulatory axis, HOXD11/CREB5/AKT/mTOR, that promotes LUAD progression both in vitro and in vivo. Targeting this pathway may represent a promising therapeutic strategy for patients with HOXD11-overexpressing LUAD.

Introduction

Lung cancer is the most common cancer globally, with an overall 5-year survival rate of approximately 20% [1]. Its pathological classification mainly includes two subtypes: non-small cell lung cancer (NSCLC)

and small cell lung cancer (SCLC), with NSCLC accounting for approximately 85% of cases [2]. Among NSCLC subtypes, lung adenocarcinoma (LUAD) is the most prevalent, with an increasing incidence and mortality rate in recent years [3]. Surgical resection is the only potential curative treatment for lung adenocarcinoma; however, due to late diagnosis, most patients miss the opportunity for this intervention. Additionally, the poor efficacy of combined treatments, resistance to traditional therapies, and high recurrence rates are significant challenges [4, 5]. Hence, understanding the molecular mechanisms underlying the occurrence and development of lung adenocarcinoma and identifying novel therapeutic targets are crucial for early diagnosis, effective clinical treatment, and improving patient prognosis.

The HOX gene (Homeobox) transcription factor family is highly conserved across different organisms [6, 7]. This family plays a critical role in regulating cell differentiation, angiogenesis, and metastasis, and is essential for cancer development [8, 9]. Dysregulated expression of HOX genes, whether as chimeric partners of fusion genes or as wild-type overexpression, has been confirmed in various solid tumors and leukemias [10–12]. In this study, we focused on the role of homeobox D11 (HOXD11) in LUAD. HOXD11, located on chromosome 2q31.1, has been implicated in tumor transformation, particularly in invasion and metastasis [13]. Overexpressed HOXD11 is a biomarker for poor prognosis in head and neck squamous cell carcinoma and glioma [14, 15]. Additionally, inhibition of HOXD11 expression in Ewing's sarcoma has been shown to limit tumor growth [16]. Our aim was to investigate the biological function of HOXD11 in LUAD and to explore its potential mechanisms in affecting tumor growth.

We demonstrated that HOXD11 directly regulates the expression of downstream CREB5 (cAMP response element-binding protein 5) as a transcription factor, which in turn regulates AKT expression, activating the AKT/mTOR pathway. This activation ultimately promotes invasive cell growth. These findings provide new insights and potential therapeutic targets for HOXD11-mediated LUAD progression.

Methods

Cell Culture and HOXD11 Genetic Manipulation

The human lung adenocarcinoma cell lines (A549, PC9, H1299, HCC827, and H1975) and the human bronchial epithelial cell line (16HBE) were obtained from China Medical University (Shenyang, China). Cells were cultured in RPMI-1640 medium (Hyclone, USA) supplemented with 10% fetal bovine serum (FBS;cytiva, Australia) and maintained at 37°C in a humidified incubator with 5% CO_2.

To achieve HOXD11 knockdown, cells were transfected with HOXD11-specific shRNA (Gene Pharma, China), using a scrambled shRNA as a negative control. Transfections were performed using Lipofectamine RNAiMAX Reagent (Invitrogen, USA) according to the manufacturer’s protocol. For overexpression, cells were transfected with a HOXD11 expression plasmid (Syngen.tech, China) or an empty vector using Lipofectamine 2000 (Invitrogen, USA). Knockdown and overexpression efficiency were confirmed by both qRT-PCR and Western blotting.

Patients, Tissue Specimens, Animals, and Research Ethics

The LUAD tissue microarray was obtained from Shanghai Outdo Biotechnology Co., Ltd. This microarray comprises 92 primary tumor specimens paired with corresponding adjacent non-tumorous tissues, totaling 170 valid cores, each with a diameter of 1.5 mm. Detailed clinical information for the patients is provided in Table 2. The use of this tissue microarray was approved by the Institutional Ethics Committee (Approval No.: SHYJS-CP-1904014). The microarray identifier is HLugA180Su08, with a chip lot number of XT19-019.

A stable A549 cell line was previously established via lentiviral transduction. For *in vivo* experiments, forty female BALB/c-nu nude mice (3 weeks old, approximately 15 g in weight) were purchased from Beijing Vital River Laboratory Animal Technology Co., Ltd. (Production license No.: SCXK [Jing] 2021-0006). The animals were housed and maintained under specific pathogen-free (SPF) conditions at the Experimental Animal Center of China Medical University Laboratory Animal Facility. The study was conducted under the guidelines and approval of the Laboratory Animal Welfare and Ethics Committee of China Medical University, approval number: CMU20231000.

Western Blot Analysis

Western blot analysis was performed to measure protein expression levels. Cells were lysed using RIPA buffer containing protease and phosphatase inhibitors. Protein concentration was determined using the BCA protein assay (Beyotime，China). Equal amounts of protein (20-40 μg) were separated by SDS-PAGE and transferred onto PVDF membranes (Millipore). Membranes were incubated with primary antibodies against HOXD11, CREB5, AKT, mTOR, p-mTOR (Ser2448), and β-actin (Supplementary Table 1). After incubation with secondary antibodies, signals were detected using ECL reagent (Beyotime，China). Densitometry analysis was performed using ImageJ software.

RNA Extraction and Quantitative Reverse Transcription-PCR (qRT-PCR)

Total RNA was extracted using the TRIzol reagent (Thermo Fisher Scientific), and cDNA was synthesized using the PrimeScript RT Reagent Kit (Takara). Quantitative PCR was performed using SYBR Green Master Mix (Takara) on an ABI 7500 Real-Time PCR System. The expression of HOXD11, CREB5, and GAPDH (internal control) was analyzed using the ΔΔCt method. Primer sequences are listed in Supplementary Table 2.

CCK-8 Assay

Cell viability and proliferation were assessed using the Cell Counting Kit-8 (CCK-8) assay (MedChemExpress，USA). Briefly, LUAD cells were seeded in 96-well plates at a density of 1,000 cells per well. After 24, 48, 72, and 96 hours of incubation, 10 μL of CCK-8 solution was added to each well. The cells were further incubated for 1–2 hours, and the absorbance was measured at 450 nm using a microplate reader (BioTek, USA). The absorbance values were used to assess cell proliferation and viability.

5-Ethynyl-2'-deoxyuridine (EdU) Assay

Cell proliferation was further evaluated using the EdU assay (Beyotime, China). LUAD cells were incubated with EdU (10 μM) for 2 hours, followed by fixation with 4% paraformaldehyde and permeabilization with 0.5% Triton X-100. After incubation with the Apollo reaction cocktail, cells were stained with DAPI and analyzed under a fluorescence microscope. The percentage of EdU-positive cells was calculated to evaluate cell proliferation.

Colony Formation Assay

Colony formation assays were conducted to assess cell survival and proliferation. LUAD cells were seeded in 6-well plates at a density of 500 cells per well and cultured for 10–14 days. Colonies were fixed with 4% paraformaldehyde and stained with 0.1% crystal violet. The number of colonies was counted, and clonogenic efficiency was calculated by dividing the number of colonies by the number of seeded cells.

Transwell Migration and Invasion Assays

Cell migration and invasion were assessed using Transwell chambers (Corning, USA). For migration assays, 1×10^5 cells in serum-free medium were seeded in the upper chamber, and complete medium was added to the lower chamber as a chemoattractant. For invasion assays, the membrane was pre-coated with Matrigel (BD Biosciences, USA). After 24 hours, the cells that migrated or invaded through the membrane were stained with HE and counted under a microscope.

Scrape Migration Assay

The scrape migration assay was performed to assess cell migration. LUAD cells were seeded in 6-well plates to reach 90% confluence. A sterile pipette tip was used to create a wound in the monolayer. Cells were washed with PBS to remove detached cells and cultured in serum-free medium. Cell migration was observed and photographed at 0, 24, and 36 hours post-scraping using a phase contrast microscope. The wound area was measured and compared.

Immunohistochemistry (IHC) and Scoring

For tissue microarray-based immunohistochemistry, the LUAD tissue microarray slides were first baked at 60 °C for 2 hours, followed by deparaffinization with xylene and rehydration through a graded ethanol series. Antigen retrieval was performed using EDTA buffer (pH 9.0) under high temperature and pressure for 3 minutes, then cooled to room temperature. For formalin-fixed, paraffin-embedded (FFPE) sections, antigen retrieval was alternatively performed in citrate buffer (pH 6.0) by boiling.

Immunohistochemical staining was performed using the MaxVision™ 2 HRP-Polymer Detection Kit (Maixin Biotech, Kit-5020, China) according to the manufacturer's instructions. After endogenous peroxidase blocking, the HOXD11and CERB5 primary antibodies were applied. Primary antibody

incubation was performed overnight at 4 °C. The next day, slides were washed with PBS and sequentially incubated with secondary reagents from the detection kit. After another PBS wash and drying, the signal was visualized using DAB chromogen solution (DAB Substrate Kit, ZSGB-BIO, ZLI-9017, China), and the reaction was terminated after 3 minutes. Slides were then counterstained with hematoxylin (Solarbio, G1080, China), dehydrated, and mounted.

Two independent researchers, blinded to the clinical data, evaluated the slides. Staining was assessed semi-quantitatively based on both intensity and percentage of positive tumor cells. The scoring system was as follows, Staining intensity: 0 = no staining, 1 = weak, 2 = moderate, 3 = strong; Percentage of positive cells: 1 = 0–25%, 2 = 26–50%, 3 = 51–75%, 4 = >76%. The final IHC score was calculated by multiplying the two subscores (range: 0–12). For further statistical analysis, a score of ≥4 was defined as positive expression, and a score <4 was considered negative expression.

RNA Sequencing (RNA-seq)

RNA-seq was performed to analyze gene expression profiles in LUAD cells with HOXD11 overexpression and knockdown. Total RNA was extracted using the RNeasy Mini Kit (Qiagen, Cat# 74104, Germany), and RNA integrity was assessed using the Agilent 2100 Bioanalyzer (Agilent Technologies, USA). Only RNA samples with a RIN value above 8.0 were used for subsequent library preparation. RNA libraries were constructed using the TruSeq Stranded mRNA Library Prep Kit (Illumina, Cat# 20020595, USA) according to the manufacturer's protocol. Sequencing was performed on the NovaSeq 6000 platform (Illumina, USA). Raw data were quality-controlled using FastQC, and adapter sequences were removed with Trimmomatic. Differential gene expression analysis was conducted using DESeq2, and results were visualized with volcano plots and heatmaps. Gene Ontology (GO) and pathway enrichment analyses were performed using the ClusterProfiler package.

Chromatin Immunoprecipitation Sequencing (ChIP-seq)

ChIP-seq was conducted to identify HOXD11-binding sites on the CREB5 promoter region. LUAD cells were cross-linked with 1% formaldehyde and lysed to isolate chromatin, which was then fragmented by sonication. Immunoprecipitation was performed using the Flag3 tag produced by Beijing Syngen Tech Co., Ltd. (Beijing, China), with the ChIP-IT Express Kit (Active Motif, Cat# 53008, USA) according to the manufacturer's instructions. ChIP-enriched DNA was purified using the QIAquick PCR Purification Kit (Qiagen, Cat# 28106, Germany), followed by library preparation with the TruSeq ChIP Library Preparation Kit (Illumina, Cat# IP-202-1012, USA). Libraries were sequenced on the NovaSeq 6000 platform (Illumina, USA). Peak calling was performed using MACS2, and binding motifs were analyzed using HOMER. Genome browser tracks were visualized with IGV.

Bioinformatics and Statistical Analysis

Bioinformatics analyses of RNA-seq and ChIP-seq data were performed using R software (version 4.2.2) and Bioconductor packages. Differentially expressed genes (DEGs) were identified using DESeq2 (for

RNA-seq) and DiffBind (for ChIP-seq). Gene set enrichment analysis (GSEA) was conducted to explore significantly enriched pathways. Gene Ontology (GO) and Kyoto Encyclopedia of Genes and Genomes (KEGG) pathway analyses were carried out to determine relevant biological functions and signaling pathways. Protein-protein interaction (PPI) networks were constructed using the STRING database.

All experiments were performed in triplicate unless otherwise specified. Quantitative data are expressed as mean ± standard deviation (SD). Comparisons between two groups were performed using the two-tailed unpaired Student's t-test, while comparisons among three or more groups were analyzed by one-way ANOVA followed by Tukey's post hoc test. The association between HOXD11 expression and clinicopathological parameters was assessed using the Chi-square test. Survival curves were plotted using the Kaplan–Meier method and compared using the log-rank test. Pearson correlation analysis was used to assess the relationship between HOXD11 and CREB5 expression. Statistical analyses were conducted using GraphPad Prism 9.0 (GraphPad Software, San Diego, CA, USA) and R software (version 4.2.2). A two-sided P value < 0.05 was considered statistically significant.

Results

HOXD11 contributes to the poor survival of LUAD

We initially conducted an analysis of HOXD11 expression in the TCGA-LUAD dataset. Our findings demonstrated that the expression levels of HOXD11 were significantly elevated in LUAD samples compared to adjacent normal tissues (Figure 1A). Additionally, in paired sample analysis, HOXD11 expression was consistently higher in cancerous tissues relative to their adjacent non-cancerous counterparts (Figure 1B). Furthermore, the prognostic significance of HOXD11 gene expression was evaluated through Kaplan-Meier survival analysis of LUAD patient samples with corresponding clinical data (Figure 1C). IHC was employed to assess HOXD11 expression in 92 LUAD samples and paired adjacent normal lung tissues using tissue microarrays (Supplementary Figure 1). HOXD11 was rarely detected in adjacent alveolar tissues (Figure 1Da) and bronchial epithelium (Figure 1Db). In contrast, HOXD11 exhibited positive expression in LUAD tissues (Figures 1Dc, 1Dd), regardless of whether the tissues were well-differentiated or poorly differentiated, with levels significantly higher than those in adjacent normal lung tissues ($P < 0.001$, Table 1). Notably, as a transcription factor, HOXD11 was predominantly localized in the nucleus. We further analyzed the correlation between HOXD11 protein expression and the clinicopathological factors of LUAD. The data revealed that HOXD11 expression was significantly associated with high T stage ($P=0.001$), lymph node metastasis ($P=0.012$), and advanced TNM stage ($P=0.001$). However, there was no significant correlation between HOXD11 expression and age ($P=0.393$), gender ($P=0.738$), or differentiation degree ($P=0.122$) in lung adenocarcinoma patients (Table 2). Moreover, as expected, elevated HOXD11 expression is indicative of a poor prognosis in LUAD (Figure 1E).

HOXD11 is overexpressed in LUAD and associated with invasive growth

Subsequently, qRT-PCR and Western blot were applied to analyze the mRNA and protein expression levels of endogenous HOXD11 in five LUAD cell lines of varying origins and biological behaviors and in normal bronchial epithelial cells. Compared to 16HBE cells, the mRNA and protein levels of HOXD11 were significantly higher in A549 and PC9 cells. Consequently, A549 and PC9 cells were primarily selected for subsequent experiments (Figure 2A, 2B). In addition, cell immunofluorescence analysis indicated that HOXD11 was predominantly localized in the nuclei of A549 and PC9 cells (Figure 2C), consistent with the IHC results from tissue specimens and the expected nuclear localization of its transcription factor role in regulating gene expression.

Next, we knocked down the expression of HOXD11 in A549 and PC9 cells (Supplementary Figure 2A, 2B) to establish stably transfected cell lines. As HOXD11 expression decreased, the number of EDU^+ cells was significantly reduced (Figure 2D), and the clonogenic ability of both LUAD cell lines was markedly diminished (Figure 2E). Consistent with these findings, the CCK-8 assay demonstrated a decreased proliferation rate in LUAD cells with reduced HOXD11 expression (Figure 2F). Transwell and scrape assays further revealed that HOXD11 knockdown effectively inhibited the invasive capabilities of the cells (Figure 2G, 2H).

To further validate the oncogenic role of HOXD11 in vivo, A549 cells with stable HOXD11 knockdown and corresponding control cells were subcutaneously injected into the flanks of BALB/c nude mice. Tumor growth was monitored over a period of four weeks. As shown in Figure 2I, tumors derived from HOXD11-silenced cells were significantly smaller in size compared to those from the control group. Quantitative analysis revealed that both tumor volume and tumor weight were markedly reduced in the HOXD11 knockdown groups (Figure 2J, 2K). Hematoxylin and eosin (H&E) staining of xenograft tumor sections revealed typical histological features of LUAD, but with reduced cellular density and mitotic figures in the HOXD11-deficient tumors, indicating a less aggressive phenotype (Figure 2L). Furthermore, IHC staining confirmed that HOXD11 expression was significantly decreased in tumors derived from knockdown cells, validating the efficacy of gene silencing in vivo (Figure 2L). These results indicate that overexpression of HOXD11 is a critical factor driving the invasive growth of LUAD.

HOXD11 transcriptionally regulates CREB5 and potentially promotes malignant phenotypes in LUAD

To further investigate the molecular mechanisms by which HOXD11 promotes the aggressive progression of LUAD, we overexpressed HOXD11 in LUAD cells (Supplementary Figure 2C, 2D) and performed integrated transcriptomic and epigenomic profiling. Specifically, RNA-seq and ChIP-seq analyses were conducted to systematically identify the downstream targets of HOXD11 and its genome-wide binding profile. RNA-seq results revealed that a total of 398 genes were upregulated following HOXD11 overexpression (Figure 3A). GO and KEGG enrichment analyses indicated that these upregulated genes were significantly associated with pathways involved in cell proliferation, mitotic regulation, and cancer-related signaling (Figure 3B). Concurrently, ChIP-seq profiling identified 15,063 HOXD11-enriched peaks across the genome, corresponding to 1,044 annotated RefSeq genes. Distribution analysis showed strong enrichment of reads around transcription start sites (TSS) (Figure

3C). Chromosomal peak mapping demonstrated widespread binding of HOXD11 across all chromosomes (Figure 3D). A pie chart summarizing the genomic localization of HOXD11 binding sites showed enrichment at promoter regions, the first intron, first exon, and intergenic regions (Figure 3E). A transcriptional regulatory network constructed from sequencing data highlighted the potential transcriptional interactions between HOXD11 and downstream genes, with HOXD11-family TFs in purple and predicted targets in red (Figure 3F). Moreover, motif analysis revealed conserved HOXD11-binding elements located proximal to the TSS regions of its targets (Figure 3G).

To identify the most relevant downstream effector of HOXD11, we intersected the top 40 differentially upregulated genes from RNA-seq with the 279 genes identified from ChIP-seq TSS-associated peaks. This analysis pinpointed CREB5 as a key overlapping target. HOXD11 was found to be strongly enriched at the CREB5 promoter region and flanking TSS sequences, indicating a direct regulatory interaction (Supplementary Table 3, 4). cAMP response element-binding protein (CREB) is a cellular transcription factor that binds to CRE, thereby regulating gene expression [17]. CREB5 belongs to the CRE family and has been reported to

be overexpressed in many types of cancer, such as ovarian cancer, lung cancer, and HCC, in which this protein orchestrates cell differentiation, proliferation and metastasis [18], and has been increasingly recognized for its role in tumorigenesis. Given this background, we hypothesized that HOXD11 may promote malignant phenotypes in LUAD through the transcriptional activation of CREB5.

Indeed, Western blot analysis confirmed that CREB5 expression was significantly upregulated following HOXD11 overexpression in LUAD cells (Figure 4A). Conversely, knockdown of HOXD11 using shRNA resulted in reduced CREB5 expression (Figure 4B). These findings further support our hypothesis that HOXD11 acts upstream of CREB5. To verify direct binding, we utilized ChIP-seq data and the JASPAR database to design primers targeting the predicted HOXD11-binding motifs within the CREB5 promoter region (Figure 4C). ChIP-PCR confirmed the enrichment of HOXD11 at the CREB5 promoter, and agarose gel electrophoresis of PCR products further validated the reliability of these ChIP-PCR results (Figure 4D). Among the predicted motifs, the site ATCATTAAT attracted particular attention. We constructed luciferase reporter plasmids containing either the wild-type CREB5 promoter or a mutant form with this motif disrupted. Dual-luciferase assays demonstrated that HOXD11 significantly enhanced promoter activity in the wild-type construct, whereas this effect was abrogated in the mutant construct (Figure 4F, 4G). These results provide strong evidence that HOXD11 directly binds to the GTCGTAAAAA motif in the CREB5 promoter to drive its transcription.

Taken together, these findings establish CREB5 as a direct transcriptional target of HOXD11 in LUAD. Through this regulatory axis, HOXD11 likely contributes to enhanced tumor cell proliferation and malignant progression.

HOXD11 promotes LUAD growth through CREB5-mediated regulation

To explore the mechanism by which HOXD11 promotes the malignant progression of LUAD, we next investigated whether CREB5, identified as a direct transcriptional target of HOXD11, mediates its oncogenic effects. We first constructed a CREB5 overexpression plasmid (Supplementary Figure 3A, 3B) and validated its efficiency in LUAD cells with stable HOXD11 knockdown. Western blot analysis confirmed that CREB5 expression was successfully restored in HOXD11-silenced cells upon transfection (Figure 5A).

We then assessed whether CREB5 overexpression could rescue the impaired proliferative and invasive phenotypes caused by HOXD11 depletion. CCK-8 assays demonstrated a significant reduction in proliferative capacity following HOXD11 knockdown, whereas CREB5 overexpression largely reversed this inhibitory effect (Figures 5B). Colony formation assays further supported these findings, as CREB5 re-expression significantly increased the number and size of colonies in HOXD11-silenced cells (Figure 5C). Moreover, functional assays of cell motility, including transwell migration and scrape assays, showed that HOXD11 knockdown suppressed LUAD cell migration and invasion, whereas CREB5 overexpression restored these capacities (Figures 5D-E). These results collectively suggest that CREB5 is a critical downstream effector of HOXD11, mediating its role in promoting LUAD cell proliferation and invasive growth.

HOXD11/CREB5 axis promotes LUAD progression via the AKT/mTOR pathway

Given that both HOXD11 and CREB5 are involved in transcriptional regulation and cell cycle control, we hypothesized that the HOXD11/CREB5 axis may drive LUAD progression through activation of key oncogenic signaling pathways. Gene set enrichment and regulatory network analysis pointed toward the AKT/mTOR pathway as a potential downstream target. Additionally, our ChIP-seq data (Figure 3D) hinted at transcriptional involvement of HOXD11 in genes associated with this pathway. To explore this possibility, we examined whether CREB5 directly regulates AKT. Western blotting revealed that CREB5 overexpression increased AKT protein levels in LUAD cells (Figure 6A). Furthermore, dual-luciferase reporter assays showed that CREB5 could significantly enhance the promoter activity of AKT (Figure 6B). ChIP-qPCR assays confirmed that CREB5 binds directly to the AKT promoter region (Figure 6C), indicating transcriptional regulation. Next, we assessed the phosphorylation status of AKT and mTOR, the two key components of the AKT/mTOR signaling axis. HOXD11 or CREB5 knockdown resulted in reduced phosphorylation of mTOR, while CREB5 overexpression rescued this reduction, restoring the activation of the pathway (Figure 6D). These findings provide mechanistic insights into how the HOXD11/CREB5 axis drives LUAD malignancy. By transcriptionally activating CREB5, HOXD11 indirectly enhances AKT expression and activation, thereby promoting mTOR signaling and contributing to increased tumor cell proliferation and invasiveness. To further verify the functional relevance of the AKT/mTOR signaling pathway in mediating CREB5-induced tumor progression, we used a pharmacological inhibitor (MK-2206 2HCl) to suppress this pathway in LUAD cells overexpressing CREB5. As expected, CCK-8 and colony formation assays confirmed that CREB5 overexpression significantly promoted cell proliferation. However, treatment with the AKT/mTOR inhibitor impaired CREB5-mediated proliferative capacity (Figures 6E-F). We further assessed its effect on cell motility.

Wound-healing and transwell assays demonstrated that blockade of AKT/mTOR signaling markedly suppressed the CREB5-induced enhancement of migration and invasion (Figures 6G-H).

So, these results suggest that the AKT/mTOR pathway plays a pivotal role in mediating CREB5-induced malignant phenotypes in LUAD. Pharmacological inhibition of this pathway can effectively attenuate the oncogenic effects of the HOXD11/CREB5 axis, highlighting the potential therapeutic value of targeting AKT/mTOR signaling in HOXD11/CREB5-high LUAD.

Discussion

LUAD, the most prevalent histological subtype of non-small cell lung cancer, remains a leading cause of cancer-related mortality worldwide. Despite recent advances in diagnostic and therapeutic strategies, the prognosis of LUAD patients remains dismal, largely due to the paucity of effective molecular targets and the complex biology underlying tumor progression [19]. In this study, we identified HOXD11 as a key oncogenic driver in LUAD and elucidated its mechanistic role in promoting tumor growth through transcriptional regulation of CREB5 and subsequent activation of the AKT/mTOR signaling pathway. HOX family transcription factors are known regulators of embryonic development and cell identity. Aberrant expression of HOX genes, including HOXD11, has been implicated in the pathogenesis of various cancers [20]. Prior studies have reported that HOXD11 exerts oncogenic effects in glioma, prostate, and liver cancers, primarily by enhancing cellular motility, invasion, and tumorigenicity [21, 22]. Our findings expand upon these observations by demonstrating that HOXD11 is markedly upregulated in LUAD tissues and cell lines, and functions as a transcriptional activator of CREB5, thereby contributing to malignant progression.

CREB5 is a member of the CREB/ATF family of transcription factors that has recently been implicated in several facets of cancer biology, including proliferation, invasion, and poor prognosis. For example, in epithelial ovarian cancer, CREB5 is upregulated in tumor tissues compared to normal tissues, correlates with advanced stage and lymph node metastasis, and its high expression is associated with shorter overall and relapse-free survival [23]. In hepatocellular carcinoma (HCC), CREB5 expression is elevated in tumor compared to adjacent liver tissue, correlates with histological grade, tumor size, vascular invasion, and worse patient survival; functional assays show that CREB5 promotes proliferation, migration/invasion, and EMT of HCC cells [24]. Additionally, in colorectal cancer, CREB5 can enhance cell proliferation, invasion, and metastatic potential, and interacts with promoters of oncogenic genes to drive these processes [25]. In the present study, we found that CREB5 is a direct transcriptional target of HOXD11, as evidenced by ChIP-qPCR and luciferase reporter assays. Functionally, silencing CREB5 abrogated the oncogenic phenotypes driven by HOXD11, underscoring its essential role in mediating HOXD11-driven tumorigenesis. Mechanistically, we demonstrated that CREB5 promotes activation of the AKT/mTOR pathway, a central signaling cascade involved in cell growth, survival, and metabolism. Overexpression of CREB5 enhanced AKT and mTOR phosphorylation, whereas its knockdown attenuated pathway activity. Notably, reintroduction of CREB5 rescued the impaired proliferative and invasive

capacity of HOXD11-silenced LUAD cells, highlighting the critical role of the HOXD11/CREB5/AKT-mTOR axis in sustaining malignant phenotypes. Our *in vivo* data further validated the oncogenic potential of HOXD11. Xenograft models revealed that HOXD11 knockdown significantly suppressed tumor growth, providing preclinical evidence that targeting HOXD11 could serve as a viable therapeutic strategy. These findings, taken together, suggest that the HOXD11/CREB5/AKT-mTOR axis represents a novel oncogenic pathway in LUAD and may serve as a promising target for therapeutic intervention.

Recent advances in drug development have led to the emergence of selective AKT and mTOR inhibitors. Several of these agents are currently undergoing clinical evaluation in patients with advanced NSCLC. For instance, sapanisertib (TAK-228), a potent dual mTORC1/2 inhibitor, has been evaluated in combination with metformin in patients with advanced solid malignancies harboring mTOR/AKT/PI3K pathway alterations. This combination demonstrated manageable safety and preliminary antitumor activity, particularly in patients with PTEN mutations and AKT/mTOR pathway alterations (ClinicalTrials.gov: NCT03017833)[26]. Similarly, gedatolisib (PF-05212384), a dual PI3K/mTOR inhibitor, has shown antitumor activity and favorable tolerability in early-phase trials involving patients with advanced solid tumors, including NSCLC [27]. Capivasertib (AZD5363), a selective pan-AKT inhibitor, is also under investigation in solid tumors, including NSCLC, with promising preliminary efficacy (ClinicalTrials.gov: NCT04308785). These efforts collectively underscore the therapeutic relevance of the AKT/mTOR pathway and highlight the potential for upstream regulators such as HOXD11 to enhance or complement current treatment regimens.

In conclusion, our study identifies a novel HOXD11/CREB5/AKT-mTOR signaling axis that drives LUAD progression. HOXD11 acts as a transcriptional activator of CREB5, leading to AKT/mTOR pathway activation and enhanced tumor growth and invasion. Targeting this regulatory axis may represent a promising strategy to improve therapeutic outcomes in LUAD. Future investigations into the development of small molecule inhibitors, siRNA-based therapeutics, or CRISPR-mediated gene editing targeting HOXD11 are warranted.

Declarations

Acknowledgments

We thank the Department of Thoracic Surgery, The First Affiliated Hospital of China Medical University and Central Laboratory of the Affiliated Central Hospital of Shenyang Medical College

Authors' Disclosures

The authors have no competing interests to disclose.

Ethics approval and consent to participate

Not applicable.

Authors' Contributions

JH. Han: Conceptualization, resources, data curation, software, formal analysis, validation, investigation, visualization, methodology, writing-original draft. CR.Jiang: Investigation and methodology. YJ Zhang: data curation, formal analysis. YF Jiang: visualization, methodology. J Ye: methodology. LD He: formal analysis, validation,

JJ Wang: visualization, methodology. S XU: Conceptualization, data curation, formal analysis, supervision, funding acquisition, validation, investigation, visualization, methodology, writing–original draft, project administration, writing–review and editing.

Funding

This research was supported by the Scientific Research Foundation of the First Hospital of China Medical University.

References

1. Siegel RL, Giaquinto AN, Jemal A. Cancer statistics, 2024. CA: a cancer journal for clinicians. 2024;74(1):12-49.
2. Krist AH, Davidson KW, Mangione CM, Barry MJ, Cabana M, Caughey AB, Davis EM, Donahue KE, Doubeni CA, Kubik M, Landefeld CS, Li L, Ogedegbe G, Owens DK, Pbert L, Silverstein M, Stevermer J, Tseng CW, Wong JB. Screening for Lung Cancer: US Preventive Services Task Force Recommendation Statement. Jama. 2021;325(10):962-70.
3. Kadara H, Choi M, Zhang J, Parra ER, Rodriguez-Canales J, Gaffney SG, Zhao Z, Behrens C, Fujimoto J, Chow C, Yoo Y, Kalhor N, Moran C, Rimm D, Swisher S, Gibbons DL, Heymach J, Kaftan E, Townsend JP, Lynch TJ, Schlessinger J, Lee J, Lifton RP, Wistuba, II, Herbst RS. Whole-exome sequencing and immune profiling of early-stage lung adenocarcinoma with fully annotated clinical follow-up. Annals of oncology : official journal of the European Society for Medical Oncology. 2017;28(1):75-82.
4. Miller M, Hanna N. Advances in systemic therapy for non-small cell lung cancer. BMJ (Clinical research ed). 2021;375:n2363.
5. Chaft JE, Shyr Y, Sepesi B, Forde PM. Preoperative and Postoperative Systemic Therapy for Operable Non-Small-Cell Lung Cancer. Journal of clinical oncology : official journal of the American Society of Clinical Oncology. 2022;40(6):546-55.
6. Gehring WJ. Homeo boxes in the study of development. Science (New York, NY). 1987;236(4806):1245-52.
7. Mallo M. Reassessing the Role of Hox Genes during Vertebrate Development and Evolution. Trends in genetics : TIG. 2018;34(3):209-17.

8. de Barros ELBR, Ramão A, Pinheiro DG, Alves CP, Kannen V, Jungbluth AA, de Araújo LF, Muys BR, Fonseca AS, Plaça JR, Panepucci RA, Neder L, Saggioro FP, Mamede RC, Figueiredo DL, Silva WA, Jr. HOX genes: potential candidates for the progression of laryngeal squamous cell carcinoma. Tumour biology : the journal of the International Society for Oncodevelopmental Biology and Medicine. 2016;37(11):15087-96.
9. de Bessa Garcia SA, Araújo M, Pereira T, Mouta J, Freitas R. HOX genes function in Breast Cancer development. Biochimica et biophysica acta Reviews on cancer. 2020;1873(2):188358.
10. Homminga I, Pieters R, Meijerink JP. NKL homeobox genes in leukemia. Leukemia. 2012;26(4):572-81.
11. Liu KY, Wang LT, Hsu SH, Wang SN. Homeobox Genes and Hepatocellular Carcinoma. Cancers. 2019;11(5).
12. Belpaire M, Taminiau A, Geerts D, Rezsohazy R. HOXA1, a breast cancer oncogene. Biochimica et biophysica acta Reviews on cancer. 2022;1877(4):188747.
13. Taketani T, Taki T, Shibuya N, Ito E, Kitazawa J, Terui K, Hayashi Y. The HOXD11 gene is fused to the NUP98 gene in acute myeloid leukemia with t(2;11)(q31;p15). Cancer research. 2002;62(1):33-7.
14. Sharpe DJ, Orr KS, Moran M, White SJ, McQuaid S, Lappin TR, Thompson A, James JA. POU2F1 activity regulates HOXD10 and HOXD11 promoting a proliferative and invasive phenotype in head and neck cancer. Oncotarget. 2014;5(18):8803-15.
15. Wang J, Liu Z, Zhang C, Wang H, Li A, Liu B, Lian X, Ren Z, Zhang W, Wang Y, Zhang B, Pang B, Gao Y. Abnormal expression of HOXD11 promotes the malignant behavior of glioma cells and leads to poor prognosis of glioma patients. PeerJ. 2021;9:e10820.
16. von Heyking K, Roth L, Ertl M, Schmidt O, Calzada-Wack J, Neff F, Lawlor ER, Burdach S, Richter GH. The posterior HOXD locus: Its contribution to phenotype and malignancy of Ewing sarcoma. Oncotarget. 2016;7(27):41767-80.
17. Mayr B, Montminy M. Transcriptional regulation by the phosphorylation-dependent factor CREB. Nat Rev Mol Cell Biol. 2001;2(8):599-609.
18. Chi Y, Gong Z, Xin H, Wang Z, Liu Z. microRNA-206 prevents hepatocellular carcinoma growth and metastasis via down-regulating CREB5 and inhibiting the PI3K/AKT signaling pathway. Cell Cycle. 2022;21(24):2651-63.
19. Zhang Y, Fu F, Zhang Q, Li L, Liu H, Deng C, Xue Q, Zhao Y, Sun W, Han H, Gao Z, Guo C, Zheng Q, Hu H, Sun Y, Li Y, Ding C, Chen H. Evolutionary proteogenomic landscape from pre-invasive to invasive lung adenocarcinoma. Cell Rep Med. 2024;5(1):101358.
20. Olatoke T, Wagner A, Astrinidis A, Zhang EY, Guo M, Zhang AG, Mattam U, Kopras EJ, Gupta N, Smith EP, Karbowniczek M, Markiewski MM, Wikenheiser-Brokamp KA, Whitsett JA, McCormack FX, Xu Y, Yu JJ. Single-cell multiomic analysis identifies a HOX-PBX gene network regulating the survival of lymphangioleiomyomatosis cells. Sci Adv. 2023;9(19):eadf8549.
21. Li B, Huang Q, Wei GH. The Role of HOX Transcription Factors in Cancer Predisposition and Progression. Cancers (Basel). 2019;11(4).

22. Huynh TLD, Ahmed R, Nasir MA, Shahbaz M, Huynh NQA. The nexus between black and digital gold: evidence from US markets. Ann Oper Res. 2021:1-26.
23. He S, Deng Y, Liao Y, Li X, Liu J, Yao S. CREB5 promotes tumor cell invasion and correlates with poor prognosis in epithelial ovarian cancer. Oncol Lett. 2017;14(6):8156-61.
24. Wang A, Yan S, Liu J, Chen X, Hu M, Du X, Jiang W, Pan Z, Fan L, Sun G. Endoplasmic reticulum stress-related super enhancer promotes epithelial-mesenchymal transformation in hepatocellular carcinoma through CREB5 mediated activation of TNC. Cell Death Dis. 2025;16(1):73.
25. Wang S, Qiu J, Liu L, Su C, Qi L, Huang C, Chen X, Zhang Y, Ye Y, Ding Y, Liang L, Liao W. CREB5 promotes invasiveness and metastasis in colorectal cancer by directly activating MET. J Exp Clin Cancer Res. 2020;39(1):168.
26. Subbiah V, Coleman N, Piha-Paul SA, Tsimberidou AM, Janku F, Rodon J, Pant S, Dumbrava EEI, Fu S, Hong DS, Zhang S, Sun M, Jiang Y, Roszik J, Song J, Yuan Y, Meric-Bernstam F, Naing A. Phase I Study of mTORC1/2 Inhibitor Sapanisertib (CB-228/TAK-228) in Combination with Metformin in Patients with mTOR/AKT/PI3K Pathway Alterations and Advanced Solid Malignancies. Cancer Res Commun. 2024;4(2):378-87.
27. Curigliano G, Shapiro GI, Kristeleit RS, Abdul Razak AR, Leong S, Alsina M, Giordano A, Gelmon KA, Stringer-Reasor E, Vaishampayan UN, Middleton M, Olszanski AJ, Rugo HS, Kern KA, Pathan N, Perea R, Pierce KJ, Mutka SC, Wainberg ZA. A Phase 1B open-label study of gedatolisib (PF-05212384) in combination with other anti-tumour agents for patients with advanced solid tumours and triple-negative breast cancer. Br J Cancer. 2023;128(1):30-41.

Tables

Table 1. The relative expression levels of HOXD11

	N	Low		High		P value
Cancer Tissues	92	44	47.80%	48	52.20%	<0.0001
Paracancer Tissues	92	82	89.10%	10	10.90%	

Table 2. Relationship between HOXD11 and Clinicopathologic characteristics

Characteristics	N	Low (N=48)	High (N=44)	P value
Age (years)				0.393
≤60	48	23	25	
>60	44	25	19	
Gender				0.738
Male	56	30	26	
Female	36	18	18	
Degree of differentiation				0.122
Well	15	8	7	
Moderate	58	34	24	
Poor	19	6	13	
Tumor status				0.001
T1-T2	69	43	26	
T3-T4	23	5	18	
N stage				0.012
N0	44	29	15	
N1-3	48	19	29	
Clinical Stage				0.001
□-□	50	34	16	
III-IV	42	14	28	

Figures

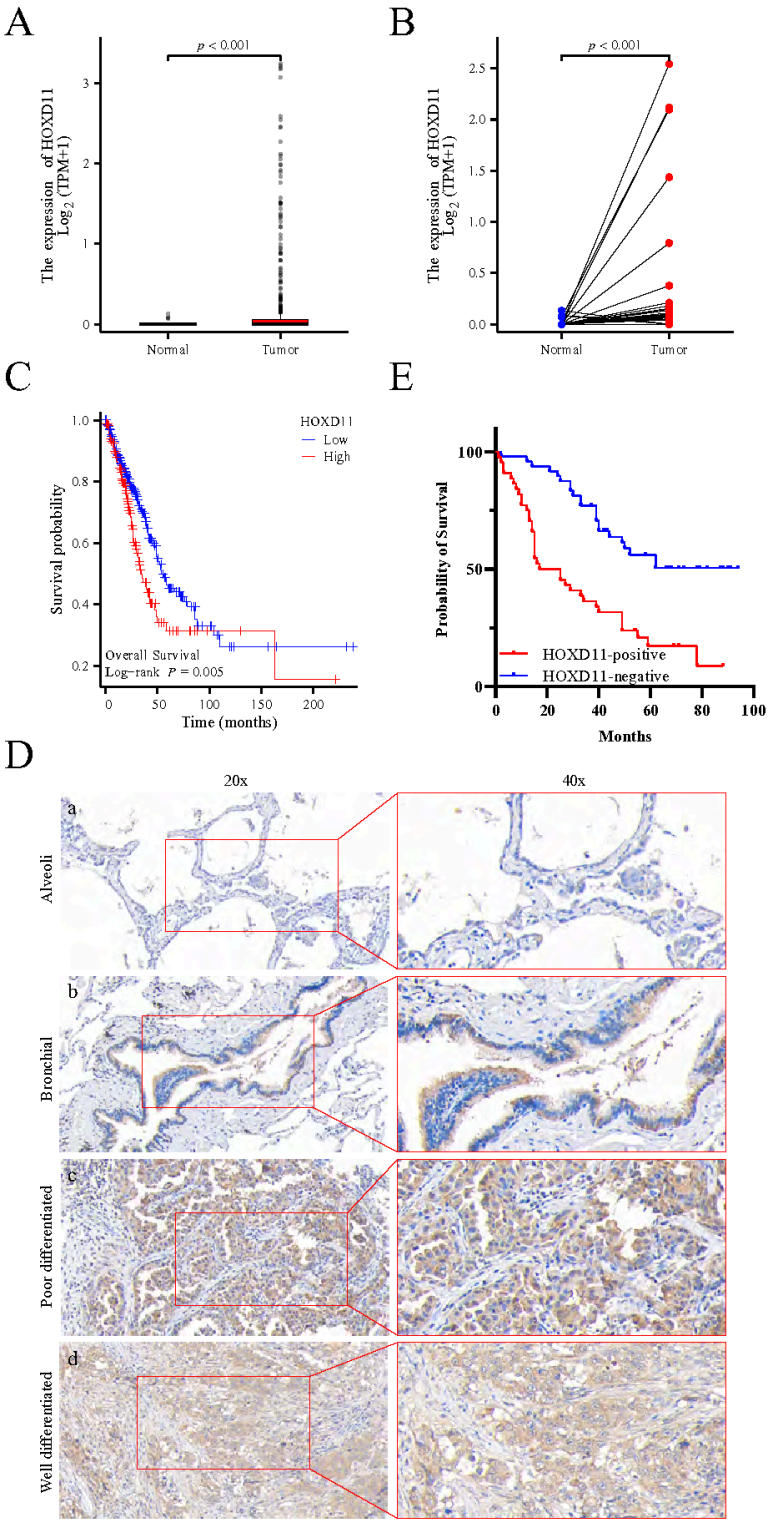


Figure 1

Legend not included with this version.

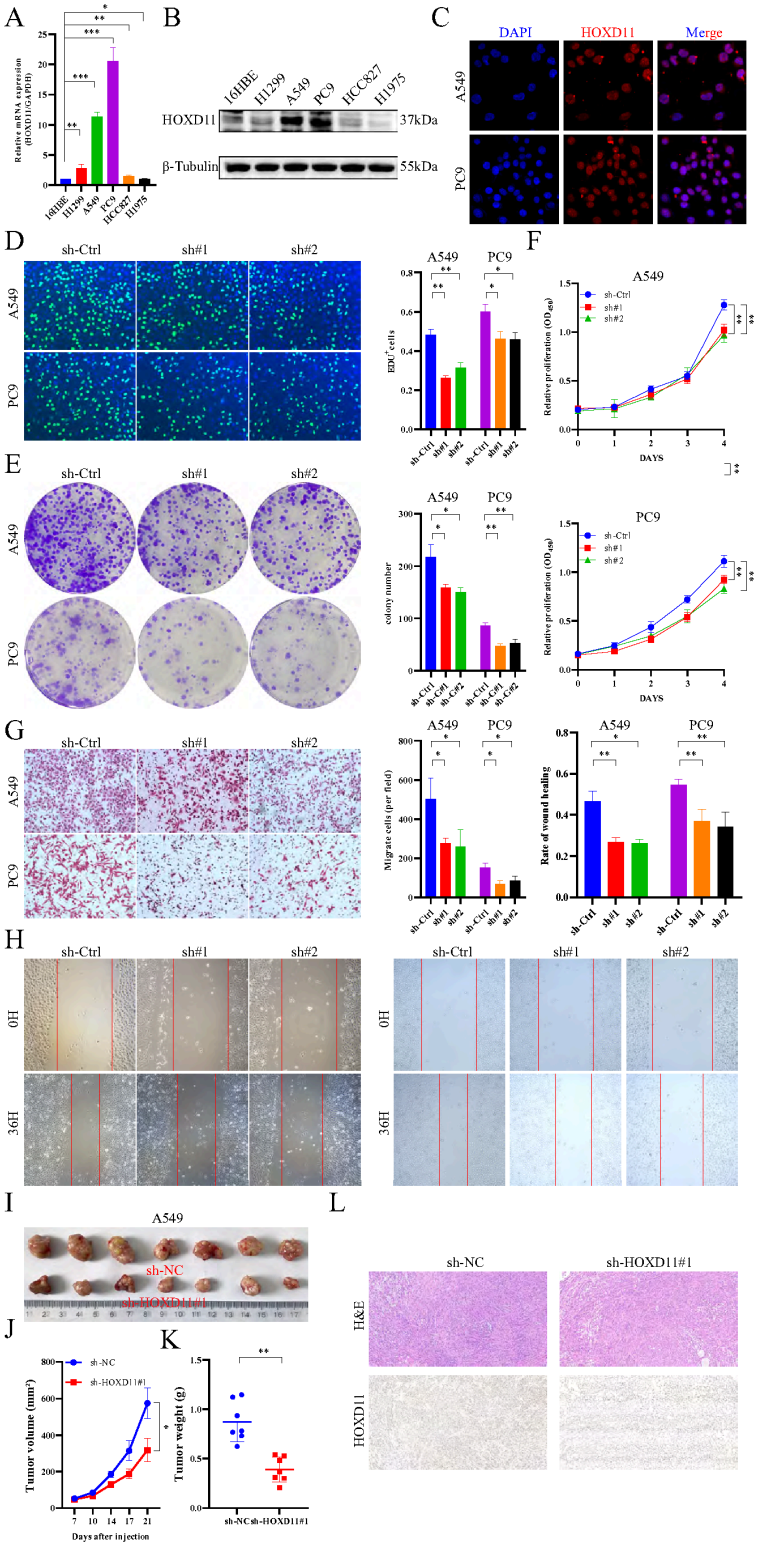


Figure 2

Legend not included with this version.

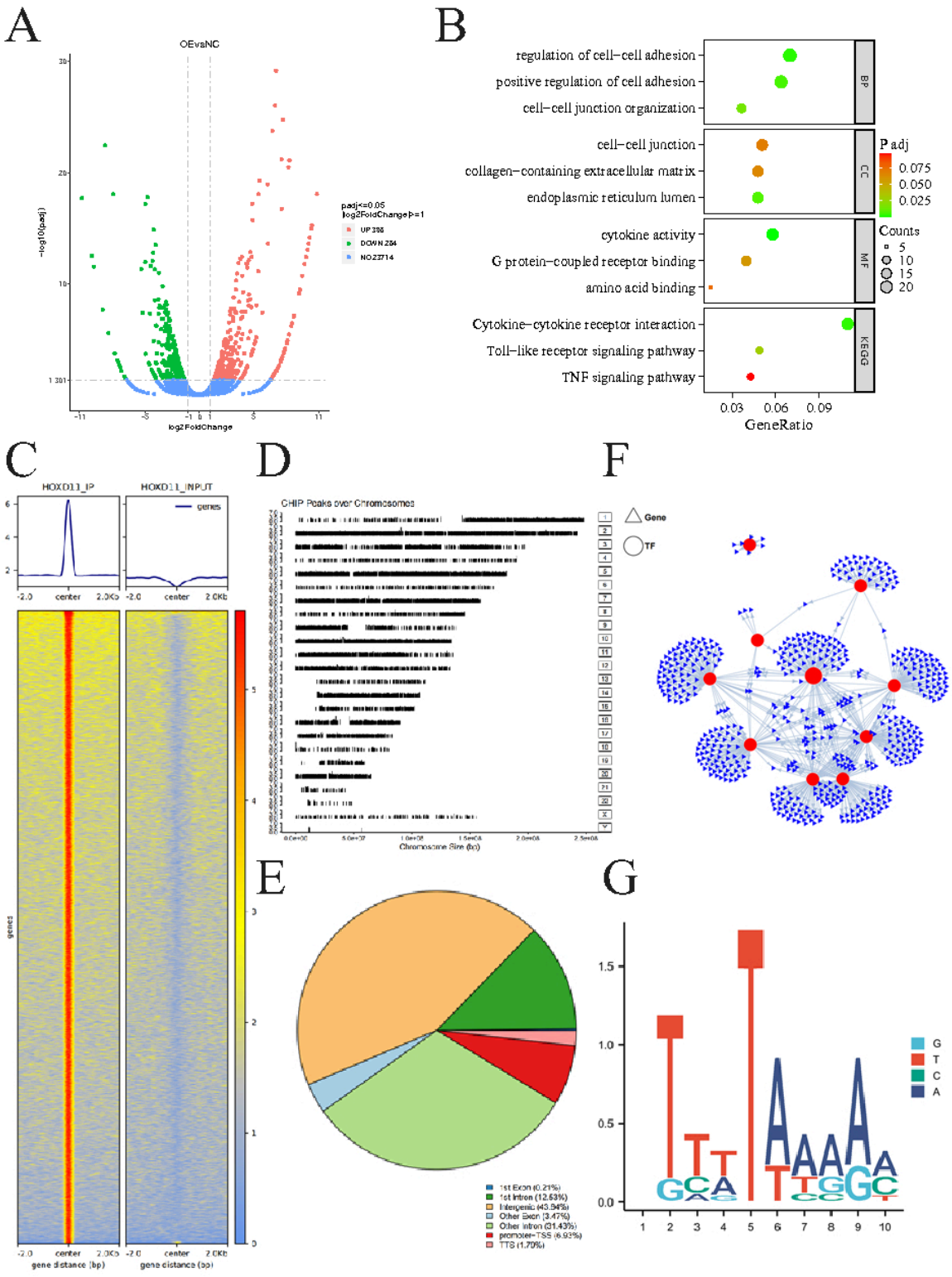


Figure 3

Legend not included with this version.

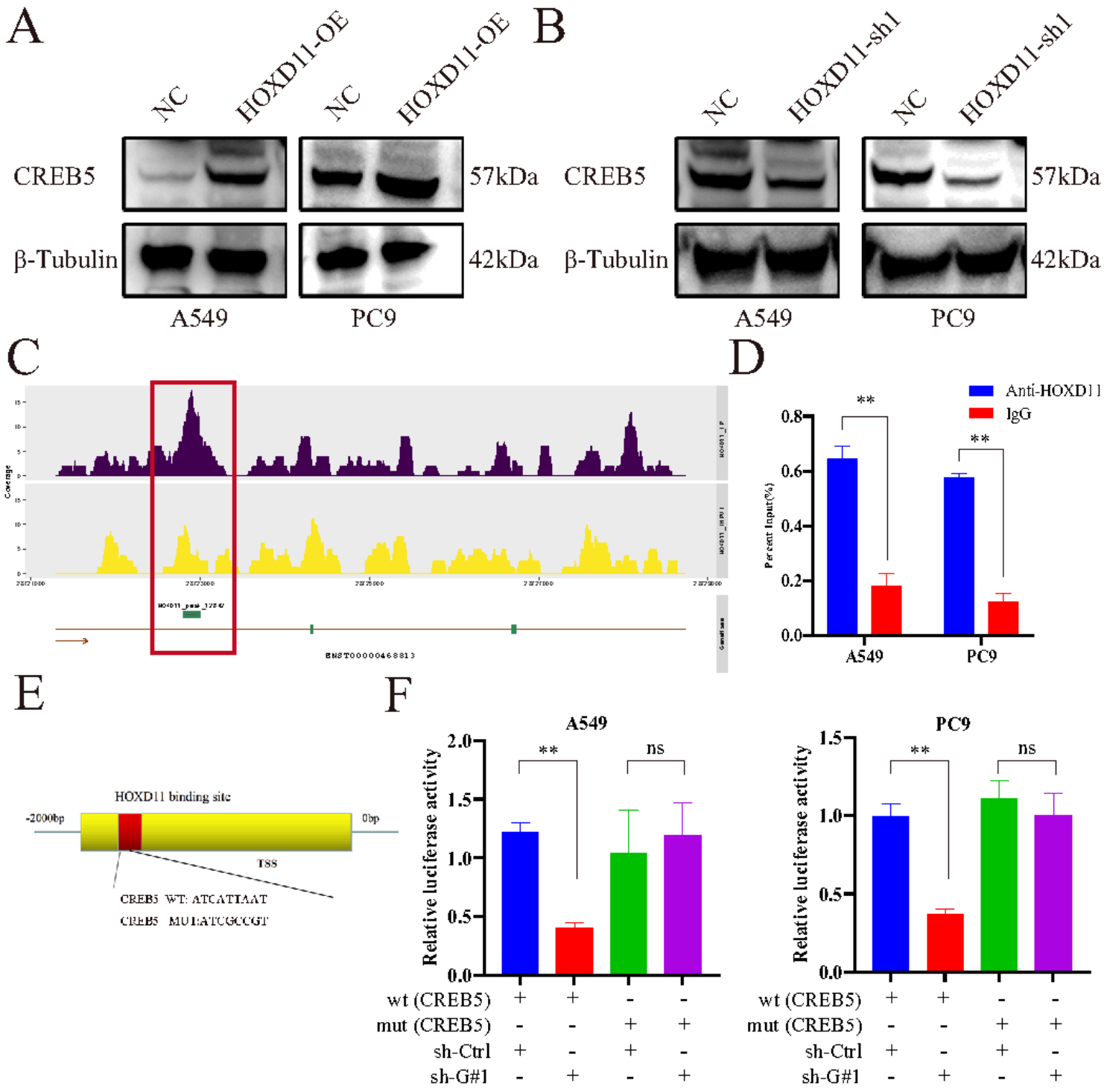


Figure 4

Legend not included with this version.

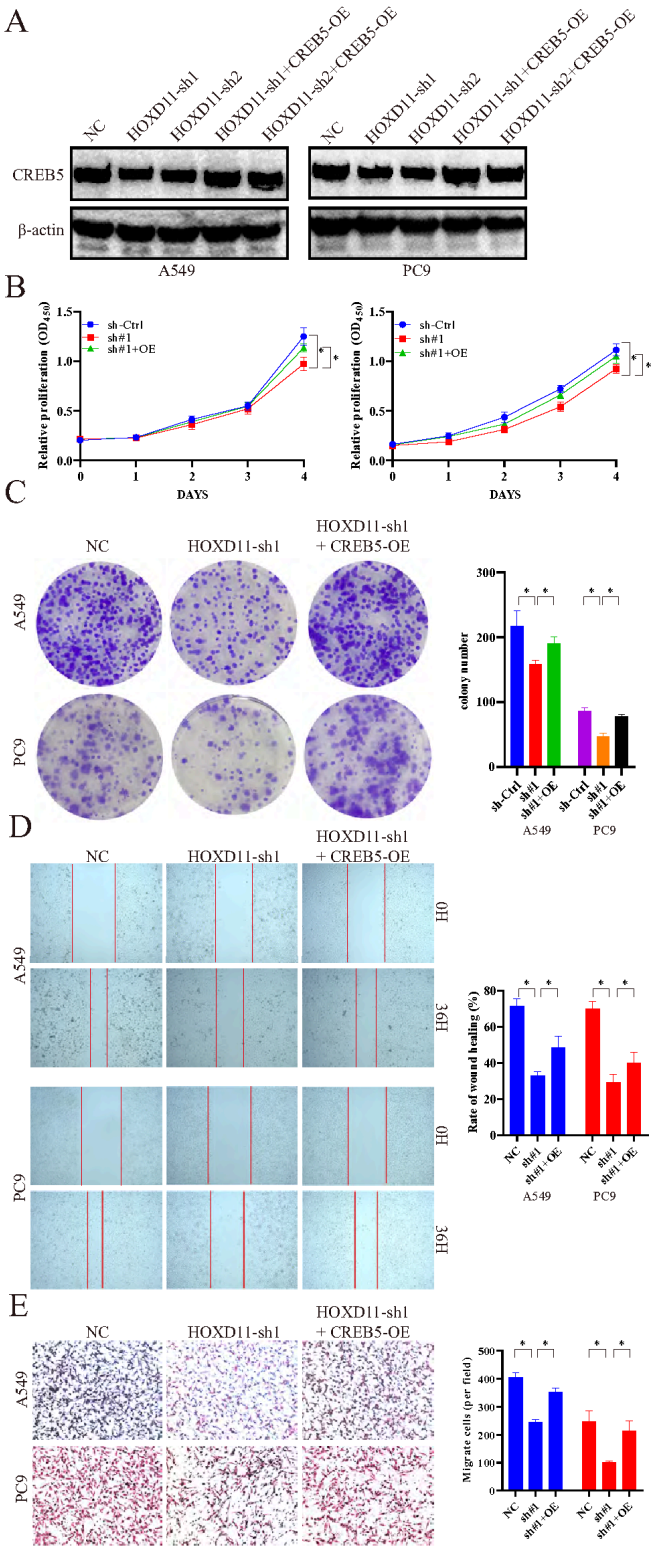


Figure 5

Legend not included with this version.

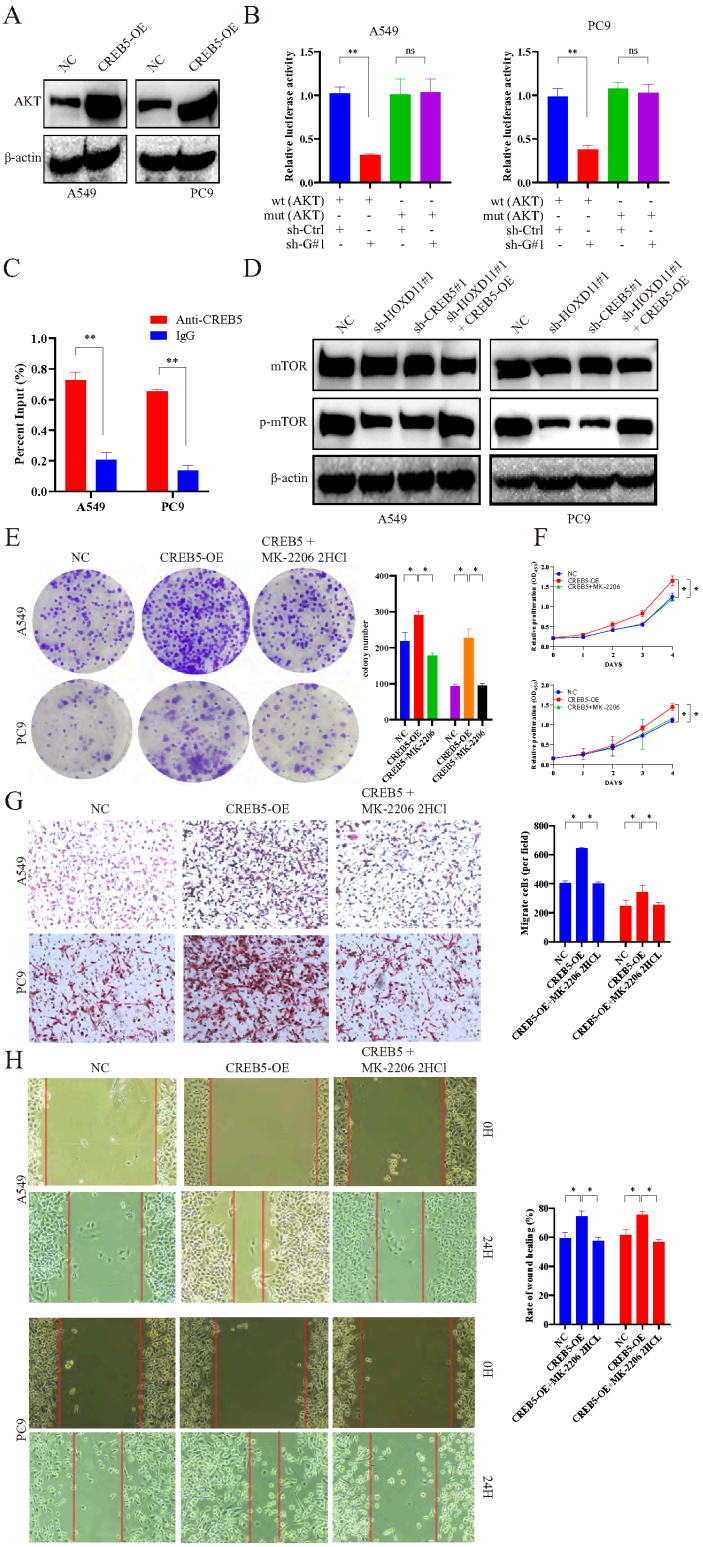


Figure 6

Legend not included with this version.

Supplementary Files

This is a list of supplementary files associated with this preprint. Click to download.

- SupTable1.docx
- SupTable2.docx
- SupFig3zip.pdf
- SupFig2zip.pdf
- SupFig1zip.pdf